Applied Surface Science Advances 7 (2022) 100201

Contents lists available at ScienceDirect

Applied Surface Science Advances

journal homepage: www.sciencedirect.com/journal/applied-surface-science-advances

Different desorption rates prompting an indirect isotopic effect on nanoscale friction

L.M. Leidens [a,*], D. Matté [a], G.L. Rech [a], J.E. Zorzi [a], A.F. Michels [a], F. Alvarez [b], C.A. Perottoni [a], C.A. Figueroa [a]

[a] Programa de Pós-Graduação em Engenharia e Ciência dos Materiais (PPGMAT), University of Caxias do Sul (UCS), Caxias do Sul, RS 95070-560, Brazil
[b] Institute of Physics "Gleb Wataghin", Campinas State University (UNICAMP), Campinas, SP 13083-970, Brazil

ARTICLE INFO

Keywords:
Friction
Isotopic effect
Phononic dissipation
Hydrogen
Deuterium
Carbon

ABSTRACT

Friction behavior at the nanoscale may be split into different contributions, including phononic dissipation. Despite the isotopic effect in the phononic component being previously explored, experimental and theoretical approaches determined contradictory conclusions. Here, a desorption-based model is proposed, and it is found to be consistent with previously published experimental data on hydrogenated and/or deuterated amorphous carbon films. Moreover, molecular dynamics simulations showed that a surface coverage difference as low as 5% might promote an effect on friction even greater than that observed experimentally. This happens when reactive defects are created after desorption (prompting carbon dangling bonds), reinforcing the assumption that minor surface differences may be sufficient for the effects observed, meeting both experimental and theoretical approaches in the same overall trend. Therefore, the phononic dissipation occurs, but the isotopic effect may be indirect, where the desorption rate of hydrogen and deuterium plays a role by exposing carbon dangling bonds, changing the interface of interaction and the nanoscale friction ultimately.

Introduction

Friction forces have attracted much attention from centuries in different areas [1], including the direct influence in the 19th century revolution on Thermodynamics, when Count Rumford proposed and performed pioneer experiments resulting in the first evidence of the production of heat by friction, influencing the nascent heat theory [2]. The non-conservative force characteristic of friction is closely related to entropy [3,4]. Indeed, a fraction of the energy involved in the work of friction forces is dissipated, which increases entropy extraction rate as in the case of a Brownian particle that walks on a discrete lattice system [5]. Otherwise, if the balance between entropy production rate and entropy extraction rate is zero, a simple walk of a macroscopic body would be impossible (due to slip at the same position). On the other hand, friction losses still represent a big issue in applications in which energy efficiency is mandatory, urging research from the nano- to the macroscale [6].

The understanding of friction at the nanoscale is still open and full of debate [7]. There are different mechanisms to describe friction at the atomic scale, where three groups are visible: phononic, electronic and van der Waals friction. Phononic friction is related to chemical bond vibration and dissipation of energy through phonons [8–10], being recently suggested as a potential channel to tune the tribological response of systems based on the materials' chemistry and geometry [11]. Electronic friction is related to electron/hole creation and electrons in conductive bands [12]. Finally, van der Waals friction is related to interatomic/intermolecular interactions at the sliding interface and it is associated with adhesion [13–15].

Phononic friction, in particular, was invoked to explain the friction behavior in hydrogenated and deuterated surfaces of carbon and silicon [16]. The isotopic effect was used to split other contributions, such as chemical bond energy, van der Waals interactions (vdW) and electronic structure. However, the isotopic effect is not only related to different vibration frequencies (phononic behavior) but also to different desorption rates of adsorbates at the sliding interface. Mo et al. [17] claimed that the isotopic effect prompting phononic friction might be mainly related to different desorption rates and coverages of hydrogen (H) and deuterium (D) on carbon surfaces. Although the work introduced new evidence against a purely isotopic effect on phononic friction (chemical bond vibration only), the actual mechanism behind the effect was not

* Corresponding author.
E-mail address: lmleidens@ucs.br (L.M. Leidens).

https://doi.org/10.1016/j.apsadv.2021.100201
Received 29 May 2021; Received in revised form 7 December 2021; Accepted 14 December 2021
Available online 28 December 2021

fully developed. Indeed, if hydrogen atoms desorb faster than deuterium ones, how does friction change? A subsequent work regarding friction behavior of C isotopes samples was published but it does not fully address this issue [18], mainly because the shift caused by the isotopic substitution is very small compared to H-D mass difference, and the reported effect on friction lies within the uncertainty of the measurement and/or simulation. One must recall that, at this moment, although experimental works concluded the existence of a direct isotopic effect for friction, theoretical approaches did not show a relationship between isotopes and friction.

In previous work, we observed that substituting hydrogen for deuterium-covered surfaces does not modify substantially the friction behavior and we also described a new component in such debate: the creation of carbon dangling bonds have a significant influence on the frictional mechanism [19]. In fact, even extrapolating the H-isotope mass to values up to 16 mass units, results corroborating Mo. et al conclusions were reported. However, when defects are created in a hydrogenated surface (replacing hydrogen adsorbates for carbon atoms with dangling bonds), small changes are sufficient for differences greater than the expected by the direct isotopes' mass [19].

In this work, we aim to introduce a hydrogen and deuterium desorption model capable of bringing new perspectives to make clearer the isotopic effect on nanoscale friction. Moreover, defects' creation effect on friction of a deuterated surface will be compared to data of hydrogenated diamond surfaces with the same content of carbon atoms with dangling bonds at the interface. Finally, we expect to integrate contradictory previously reported behaviors from experimental and theoretical approaches in the same overall trend.

Materials and methods

The methodology is divided into two groups: (i) a first group, where a desorption model is developed to explore the different desorption rates of isotopes on surfaces, and (ii) a second group, where molecular dynamics (MD) simulations were performed to evaluate friction forces in similar surfaces as those obtained in the desorption model when reaching the steady-state.

An insight regarding different hydrogen and deuterium desorption rates was the primary idea used to develop this work, where the difference in C-D and C-H zero-point vibrational energy (ZPE) is mostly responsible for isotope-dependent phenomena [20]. To quantitively access the effect, a thermo-activated process of bonding-break at the interface following a Boltzmann distribution was considered, as already suggested in other nanotribological analyses [21]. The fundamental constants and materials' properties used in the calculations were obtained in the bibliography and cited where they were used. In order to compare the theoretical approach with consolidated experimental results, tribological and physicochemical data on material systems published elsewhere [22,23] was also considered. In such work, amorphous carbon thin films deposited on Si (100) substrates with a developed methodology [24] using plasma enhanced chemical vapor deposition (PECVD) with RF power supply (13.56 MHz) and different mixtures of methane (CH_4) and deuterated methane (CD_4). Such an approach resulted in samples with different contents of hydrogen and deuterium. These samples were evaluated by lateral force microscopy (LFM) in order to explore the nanofriction behavior variation with the different isotopes' content. The input data for the calculations using the proposed model comes from these published experimental works, namely the chemical composition and temperature. A ratio analysis was proposed to compare results from different samples relative to the more hydrogenated specimen, considering the uncertainty of the experimental results. With such an approach, it is possible to quantify and infer the D substitution's effect on friction compared to a non-deuterated surface in conditions consistent to the experimental setup. Since the desorption is a thermo-dependent event, the analysis was, finally, extrapolated to a set of temperatures to complement the discussion in different conditions.

Additional data was obtained by MD simulations using the Large-scale Atomic/Molecular Massively Parallel Simulator (LAMMPS) with the adaptive intermolecular reactive bond order (AIREBO) potential to investigate the effect of dangling bonds at the sliding interface for both H- and D-passivated flat [111] single-crystal diamond surfaces. Long-range van der Waals interaction contributions are included in the interatomic potential. The crystallographic surface used in our simulations was chosen to be similar to that used by Cannara et al., in experimental friction measurements by AFM [16], and Mo et al. in simulations [17]. Since the computational setup is well controlled and the temperature was maintained constant at 10 K, it was possible to avoid interference from different phenomena and adequately analyze the effect of different surface coverages on friction. The setup was similar to the one used in our previous work [19], consisting of a probe and a substrate in a mirrored-condition, with three distinct regions: (a) the bottom region (one atom-thick layer treated as a rigid plate after the relaxation of atomic positions), (b) the NVT (canonical ensemble with constant particle number, system volume, and temperature) ensemble at 10 K consisting of five atomic layers coupled to a Nose-Hoover thermostat with friction factor of 0.5 ps, and (c) the top region of four atomic layers in the NVE (microcanonical ensemble, with constant particle number, system volume, and total energy) ensemble. Namely, the sample consists of a flat slab of 14.14 nm by 14.46 nm and 2.09 nm thick and the probe is formed by a flat 2.5 nm x 2.6 nm x 1.7 nm. The bottom rigid atomic layer of the sample is used to drag the whole system with a constant velocity of 1 Å/ps in the [11] crystallographic direction. A spring of constant 3 eV/Å is attached to the rigid top layer of the probe in the direction opposite to the direction of movement of the sample. A schematic of the setup used during the MD simulations is presented in Fig. 1. The normal force was fixed constant and equal to 33 nN in all the simulations. After the initial energy minimization, the system was let to equilibrate for 6 ps (60,000 steps), after which the relative movement of the sample begins. The system is then let to evolve for a time between 2.6 and 42 ps until it reaches a steady-state condition, i.e., when the average of the instantaneous lateral force on the spring and the temperature of the NVE region remained constant. Once the system is in a steady-state regime, the

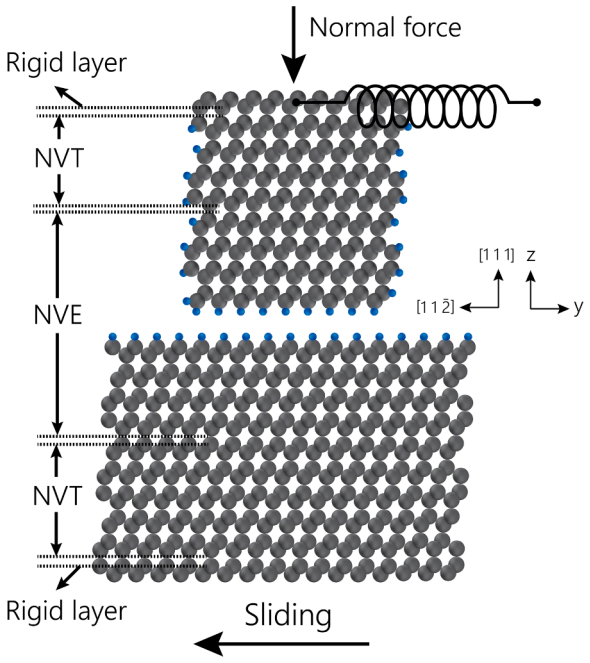

Fig. 1. Schematic of the system used in MD simulations, consisting of a diamond probe (on top) and part of the diamond substrate, both divided in NVE and NVT regions, and a rigid layer. A spring is attached to the rigid top layer of the probe in the direction opposite to the direction of movement of the sample.

production phase begins and lasts for a minimum of 36 ps in order to sample at least four friction force cycles. Each simulation had a total of 6,000,000 timesteps and we used a timestep of 0.1 fs. Both body (sample) and counter-body (probe) surfaces were passivated with H atoms, acting as the adsorbates at the interfaces. In order to explore the mass effect on the phononic component, the mass of the H atoms on the diamond surface was artificially changed from 1 u (H) to 2 u (D), while keeping the interatomic potential unaltered. The effect of possible desorption events of the adsorbates was verified by replacing 2% and 5% of the H and D atoms with C atoms with dangling bonds in both sample and probe surfaces, and comparing the results with the unaltered condition (full coverage). Hydrogen-covered surfaces' results from our previous work [19] were, finally, compared to the deuterated surfaces here simulated. Additionally, we obtained the vibrational modes of the C-H (-D) bonds from the Fourier transform of its velocity autocorrelation function. Although certain parameters values are higher than the average used in experimental setups, such as the sliding velocity, and this a current issue in computational setups the only variable in the simulations is the H-isotope mass. Moreover, the velocity used is much smaller than the speed of sound in diamond, suggesting that such a parameter it is not a limiting factor in the phononic energy dissipation and, consequently, possible effects based on this phenomenon would be identified. Data analysis of the MD simulation results was implemented using Jupyter notebooks [25] with Python language. Curve fittings and analysis were performed using the LMFIT [26] and UNCERTAINTIES [27] packages.

Results and discussion

The desorption rate from surfaces (R_x) may be expressed as in Eq. (1), where θ_x is the coverage fraction of the atom x on the surface, with $\theta_x = \sigma_x/\sigma_T \approx [x]_{surface}$ with σ_x and σ_T being, respectively, the actives sites occupied by an atom x and the total number of available active sites. Here, x = H or D, since surfaces passivated by H and/or D are considered.

$$R_x = \frac{d\theta_x}{dt} = K_{d_x} \cdot \theta_x \tag{1}$$

The desorption constant (K_{d_x}), representing the bond breaking and a thermo-activated process, follows a Boltzmann distribution, mostly known as Arrhenius law, as presented in Eq. (2). K_{O_x} stands for a frequency, *i. e.*, the number of attempted escapes per second and, here, approximated by ω_{O_x} (fundamental stretching vibration frequency of the bond considered), and ε_{d_x} is the energy barrier for desorption. A similar thermo-based approach was previously suggested [21] to describe atomistic wear in single asperity contacts during AFM measurements.

$$K_{d_x} = K_{0_x} \cdot e^{-\varepsilon_{d_x}/kT} \tag{2}$$

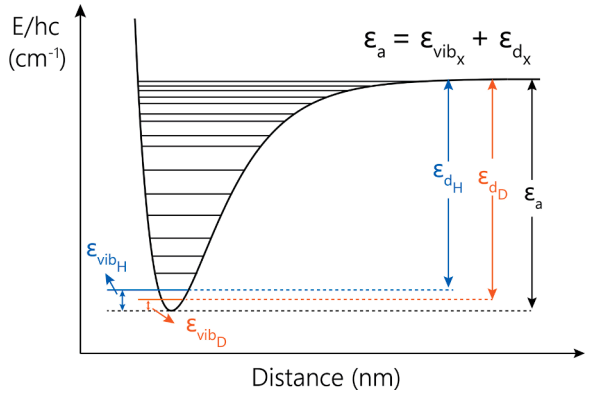

Fig. 2. Schematic of vibrational ground-state electronic levels for C-H and C-D bonds

Considering the scheme of Fig. 2, with the vibrational ground-state electronic levels [28] for C-H and C-D bonds, it is possible to define the ground-vibrational-state dissociation energy (or energy barrier for desorption) ε_{d_x} and the equilibrium dissociation energy ε_a for C-H and C-D bonds. The zero-point vibrational energy (ZPE or ε_{vib_x}) for the bonds is different and, since ε_a is considered, at this point, barely equal, there is also a difference in ε_{d_x}.

For the case expressed above, ε_a is defined by a non-harmonic oscillator, as determined in Eq. (3).

$$\varepsilon_a = \varepsilon_{d_x} + \left(\frac{1}{2}\right)h\nu_x - \left(\frac{1}{4}\right)h\nu_x x_x \tag{3}$$

However, it is possible to approximate the condition of the ZPE as a harmonic oscillator and the equation is simplified, as reported in Eq. (4).

$$\varepsilon_a = \varepsilon_{d_x} + \left(\frac{1}{2}\right)h\nu_x = \varepsilon_{d_x} + \varepsilon_{vib_x} \tag{4}$$

Therefore, ε_{d_x} for a particular bond may be expressed as presented in Eq. (5).

$$\varepsilon_{d_x} = \varepsilon_a - \varepsilon_{vib_x} \tag{5}$$

By rearranging Eq. (2), considering Eq. (5), K_{d_x} may finally be expressed as

$$K_{d_x} = \omega_{0_x} \cdot \frac{e^{(\varepsilon_{vib_x})/kT}}{e^{(\varepsilon_a)/kT}} \tag{6}$$

where k is the Boltzmann constant ($k = 0.008314\ kJ{\cdot}mol^{-1}{\cdot}K^{-1}$) and T is the absolute temperature. The vibration frequency and energies are presented in Table 1 for both C-H and C-D bonds [23,28–32]. One can note that ε_{a_H} and ε_{a_D} were considered as equal in a first approximation. In fact, ε_{a_H} and ε_{a_D} are slightly different and, for this reason, the actual values from [29] were used in the following calculations. With x = H or D, Eqs. (7) and (8) give the desorption rates for H and D, respectively.

$$R_H = \frac{d\theta_H}{dt} = K_{d_H} \cdot \theta_H \tag{7}$$

$$R_D = \frac{d\theta_D}{dt} = K_{d_D} \cdot \theta_D \tag{8}$$

Since the surfaces may present different coverages of H and/or D, the desorption mechanism may be evaluated as a combination of independent events of both atoms in time. In the case of surfaces covered by different amounts of hydrogen and deuterium, the total desorption rate is expressed in Eq. (9).

$$R_T = (R_H + R_D) = \frac{d\theta_H}{dt} + \frac{d\theta_D}{dt} \tag{9}$$

For a better comparison of a set of samples, it is possible to calculate a ratio between the total desorption rate of each sample and the desorption rate of the sample with the highest hydrogen content. As given in Eq. (10), the ratio expresses the relative desorption rate of a sample i compared with the highly hydrogenated sample of a set, at the same time interval.

$$Ratio = \frac{R_{T_i}}{R_{T_{H_{max}}}} = \frac{(d\theta_{Hi}/dt) + (d\theta_{Di}/dt)}{(d\theta_{Hmax}/dt)} = \frac{(K_{d_H} \cdot \theta_H)_i + (K_{d_D} \cdot \theta_D)_i}{(K_{d_H} \cdot \theta_H)_{max}} \tag{10}$$

Using this approach, it is possible to directly compare the trend of

Table 1
Vibrational frequencies and energies calculated for C-H and C-D bonds, with data from [23,28–32].

	Stretching modes (ω_{0_x})		ε_{vib_x}	ε_{d_x}	ε_a
	(cm^{-1})	(s^{-1})	($kJ \cdot mol^{-1}$)	($kJ \cdot mol^{-1}$)	($kJ \cdot mol^{-1}$)
C-H	~ 3000	$8.99 \cdot 10^{13}$	17.94	338.40	356.34
C-D	~ 2250	$6.75 \cdot 10^{13}$	13.46	341.40	354.86

experimental results of friction with the model's results. The experimental set of results used for comparison came from Echeverrigaray et al. [22], where amorphous carbon thin films samples with different H and D contents had their nanotribological properties accessed by LFM. Table 2 presents the atomic content of the samples, as reported in the work and used to the here proposed calculation.

In order to apply the model, θ_x for each sample was approximated as the atomic fraction of H and D, respectively, as previously indicated. Similarly, the ratio is calculated for the friction forces (F_F) obtained experimentally, as presented in Eq. (11).

$$Ratio = \frac{F_{F_i}}{F_{F_{Hmax}}} \tag{11}$$

Additional energy from the contact pressure, as proposed in [21], was not evaluated since it is considered constant because of similar physicochemical and mechanical properties of all the samples and equal sliding parameters, as reported in [22]. Therefore, the ratio used to evaluation cancels such a constant contribution. Fig. 3 presents the comparison between the model and the experimental results for samples considering the atomic coverages of theoretical surfaces equal to the fraction of H and/or D and the sample of 20 at. % of H (and 0 at. % of D) as the condition of maximum desorption, because it is the most hydrogenated sample.

Firstly, one can note a monotonic decreasing behavior of the calculated ratios for the theoretical approach. It means that the higher the deuterium coverage content, the lower desorption rate of the adsorbed atoms. Secondly, the friction force ratio also decreases monotonically as a function of deuterium content following the same trend as for the desorption rate ratio, considering the experimental uncertainty. The small change on ε_{vib_x} may result in such an effect, as also explored experimentally by Figueroa et al. [33] for surface hardness increasing of iron alloys, where the reduction of the ZPE leads to a lower scission energy of hydrogen-metal bonds as compared with deuterium-metal bonds. Indeed, such a property based on the isotopic difference is also a key tool for other applications, with the known kinetic isotope effect (KIE) [20,34], and was even reported as the actual mechanism regarding the isotopic effect in friction by Mo et al. [17] contrasting experimental results from [16], which considers the atomic mass as the critical parameter to such an effect. When experimental data is added for comparison, it is possible to note that the trend is similar within uncertainty and present agreement with the model, considering the body of experimental data previously reported. Deviations are expected since the experimental data are totally independent of the model, which only evaluates a possible difference in desorption rates, *i. e.*, the experimental results may depend on other intervening effects. Therefore, based on a direct comparison, the difference on the desorption rates seems to have a relevant role describing the effect for the conditions here studied, backed by experiments.

As presented in Eq. (2), desorption is a thermo-dependent process. Therefore, it is also possible to evaluate the ratio in function of the temperature of the system/ambient. Fig. 4 shows the theoretical ratios, also calculated with Eq. (10), for a set of temperatures, including the temperature similar to the experimental tests (298 K).

The monotonic decreasing with the increasing in the deuterium content on surface is maintained in all the cases, although a difference is noted: as the deuterium content increases, the dispersion of desorption rate increases. This result indicates that the difference caused by desorption may be smaller at higher temperatures, but it is still present and representative. One can note that the slope of a hypothetical line passing on the points of each temperature would decrease with the increasing of the temperature, remarking that the relative desorption difference decreases with the temperature. Therefore, for samples passing through annealing processes, the difference may be smaller, but still consistent and relevant for temperatures up to 800 K. On the other hand, when the temperature is much smaller, the effect may be even more evidenced as visualized in the scenario with 65 K. The relative desorption of D when compared to H is very close to zero, because desorption is hampered in such a temperature for both atoms and if only a small amount of H is desorbed, the D desorption may be almost hindered. The more deuterium is present, the bigger the weight of less deuterium desorption rate. Deuterium needs more thermal energy to desorb.

In order to complement the results and enhance the understanding on how the desorption process possibly affects the friction behavior, MD simulations were carried out to evaluate the defects' creation effect (to

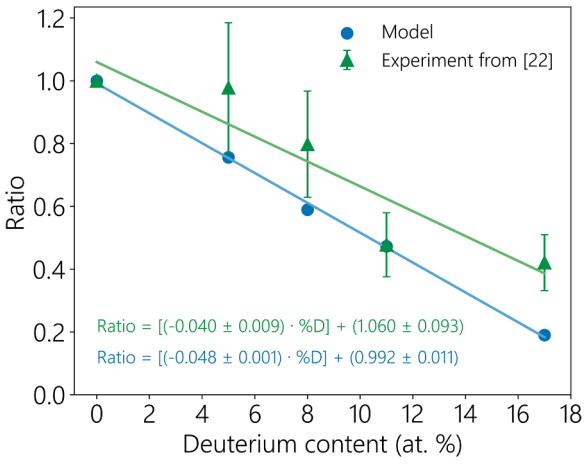

Fig. 3. Comparison between the theoretical model considering the difference of desorption rates for surfaces with different H/D coverages and experimental data for similar surface accessed by LFM, previously reported in [22]. Ratios are used to directly compare the model with friction data obtained experimentally. The equations for both linear regressions are presented at the left corner, with R^2 equal to 0.998 and 0.857 for the theoretical and experimental data fitting, respectively.

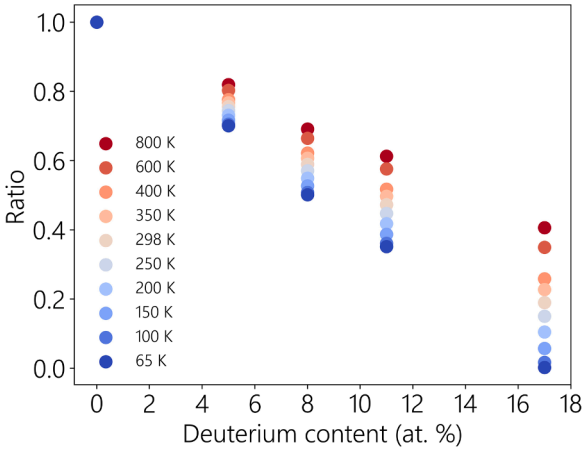

Fig. 4. Ratios obtained with the theoretical model proposed for desorption rates considering different temperatures, from 65 to 800 K

Table 2
Atomic composition of the samples used in experiments, as reported in [22,23] and used for comparison with the proposed model.

Sample	H (at. %) ≈ (θ_H · 100)	D (at. %) ≈ (θ_D · 100)
(i)	20	0
(ii)	14	5
(iii)	10	8
(iv)	7	11
(v)	0	17

correlate with desorption) on friction for diamond surfaces covered with hydrogen and deuterium, using an interatomic potential including vdW interactions at the interface. The systems were described following the methodology presented in the Materials and Methods section to assure that the surface is covered with the exact adsorbates' percentage determined in each condition, without recovery or additional desorption/adsorption.

Fig. 5 shows the vibrational density of states (VDOS) of the diamond surface passivated with hydrogen for isotope masses of 1 u and 2 u (H and D, respectively) obtained from the velocity autocorrelation function of the explored MD simulations. One can note that the systems' vibrational dynamics are adequately captured by the simulations since the contribution assigned to the C-H stretching mode, near 3000 cm^{-1}, is evidenced. Moreover, this peak is shifted to a lower wavenumber for an isotope with mass equal to 2 u, as expected for a deuterium. The results agree with the vibrational characteristics from experimental data of similar materials, including the actual samples used to compare with the model [23,30,32]. Since MD simulations capture the system's vibrational dynamics, it can be inferred that friction data may reflect any possible direct phononic effect.

In order to explore the difference in friction associated with different surfaces' coverages and density of defects (carbon atoms with dangling bonds replacing H/D at the interface), Fig. 6 presents the friction force between sliding for diamond surfaces totally and partially covered by hydrogen isotopes with atomic masses of 1 or 2 u (to compare H and D frictional behavior, respectively), under a normal load of 33 nN. Firstly, one can note that, in identical coverage conditions, it is possible to affirm that H- and D-passivated surfaces exhibit the same friction forces, as the results are within the uncertainty with a 0.05 significance level. However, considering a slight difference of 5% in surface coverage, the results are indeed different, with greater friction for a less passivated surface, it is, with more carbon atoms with dangling bonds available at the interface for both H and D covered surfaces. Such a small coverage difference is possible, since our model and previous works point to a difference of desorption rates as high as two times greater for hydrogenated surfaces [33], which is larger than the isotopic effect in nanoscale friction published by Cannara et al. [16] and De Mello et al. [23], of about 35%. In the simulation, the condition is totally controlled to active carbon atoms replace the H or D atoms, it is, the carbon atom preserves the dangling bond after cleavage. This can be assured because all simulations here discussed were carried out at a temperature of 10 K, i.e., under a condition which hinders surface reconstruction and additional desorption/adsorption. These results agree with our previous work [19] and inferences published by Mo et al. [17]. Additionally, Fig. 7 shows raw traces of the instant friction forces in function of the sliding for both surfaces, in conditions of total coverage (100%) by the

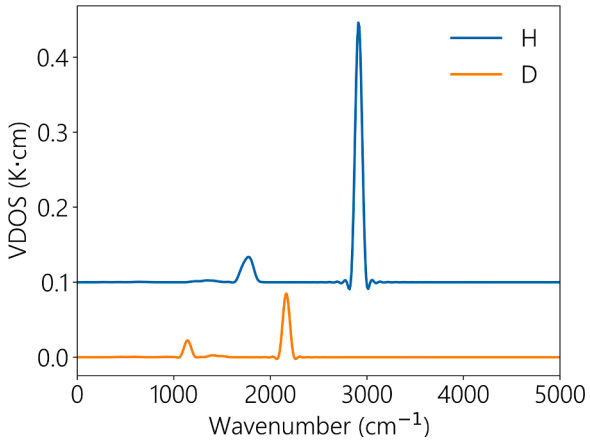

Fig. 5. Vibrational density of states (VDOS) for both surfaces as obtained from MD simulations of H (mass 1 u) and D (mass 2 u) passivated diamond surfaces.

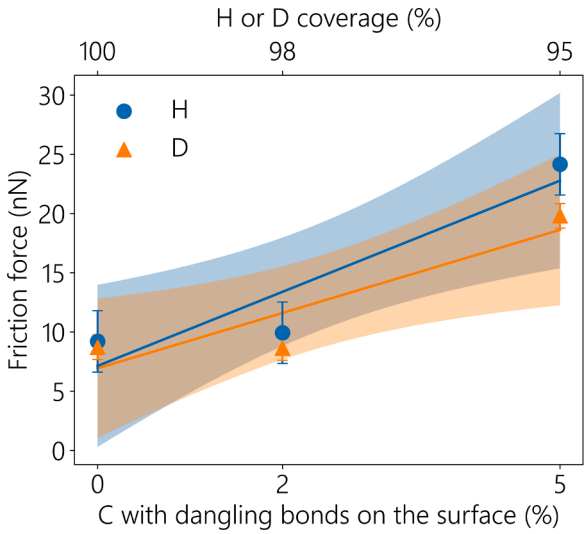

Fig. 6. Friction force between obtained in MD simulations for diamond surfaces totally and partially-covered by H isotopes atoms with atomic masses of 1 and 2 u to compare H and D frictional behavior, respectively, under a normal load of 33 nN. Data from hydrogenated samples were obtained from a previous work [19] and compared with the deuterated surfaces' MD simulations. The H/D atoms in the passivation layers in both sliding surfaces were gradually replaced by carbon atoms with dangling bonds in order to simulate the condition after adsorbate desorption. Blue and orange bands represent the 95% confidence prediction intervals for H- and D-passivated surfaces friction forces, respectively

adsorbates and partial defect creation (5%) for (a) H and (b) D, respectively. One can note that in the condition of total passivation both surfaces present similar results, with stick-slip sliding, independent from the isotope mass. However, when H or D atoms are replaced by active defects, the behavior changes. The friction force may be linked to the presence of carbon atoms with dangling bonds ate the interface (a possible consequence of the desorption of adsorbed specimens). Therefore, even a small content of non-passivated carbon atoms may lead to a substantial difference in the friction forces of such a system. Similarly, when the conditions of 95% to both adsorbates are compared, no clear difference is evidenced: the results are similar both quantitative and qualitatively, as evidenced in Fig. 6. One can additionally note that the pure stick-slip behavior observed to the fully passivated samples is transitioned to a state with more fluctuations of the instantaneous friction forces. This change may be directly associated with the active interaction of the atoms with dangling bonds at the interface, leading to higher friction forces and more dispersion of the results.

An experimental and theoretical paper [35] recently explored the interaction of different atomic terminations on graphene steps resulting in different friction behaviors when dangling bonds are present at the interface, if compared to passivated surfaces and/or with smooth paths. It may be inferred that, under experimental conditions (where it is not possible to totally control the surface coverage like in MD simulation with ultra-low temperatures), this effect may be also linked to the increase of friction if the experimental setup is not under ultra-high vacuum, for example. Since passivation of the created dangling bonds with molecules at the working atmosphere may take place (with water or other oxygenated molecules, for example) it may diminish the hydrogen/deuterium effect of lowering the friction forces. Therefore, when fewer bonds are broken (with higher D contents and, consequently, minor desorption rates), less carbon atoms with dangling bonds are available at the interface, less substitution reactions take place, and the friction force is lower. This hypothesis is also sustained by Mo et al. [17] work, reinforcing that the isotope effect on solid friction is possibly due to the chemical stability of surface-termination. Fig. 8 shows a schematic of the mechanism proposed for (a) hydrogenated, (b) hydrogenated-deuterated, and (c) deuterated samples without posterior

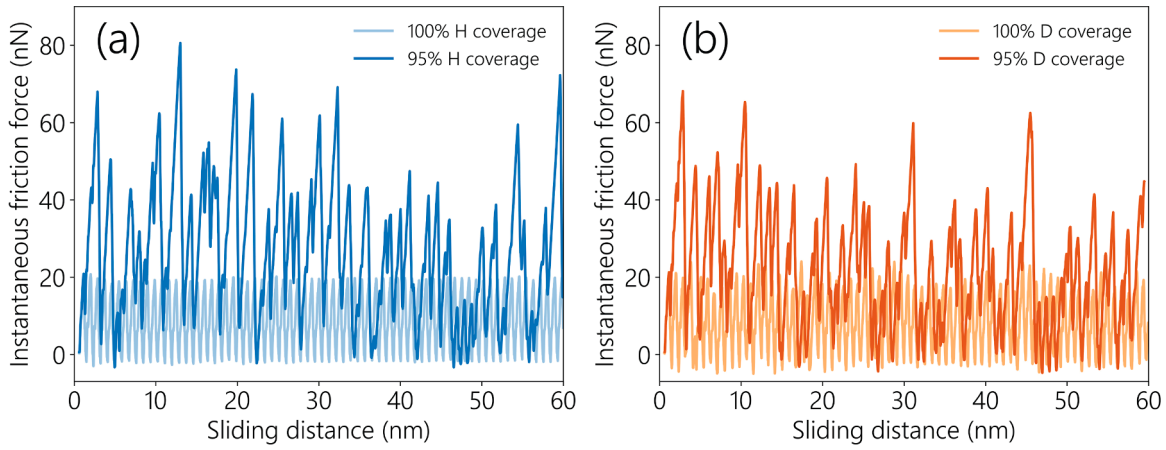

Fig. 7. Raw traces of instantaneous friction forces for both (a) hydrogenated and (b) deuterated-diamond surfaces during MD simulations. Two conditions are presented: a fully passivated surface and a surface with 5% of defects (carbon atoms with dangling bonds). A clear difference is noted between the conditions of a similar surface, however, between the samples with difference isotopes as adsorbates, the trend is similar both qualitative and quantitatively.

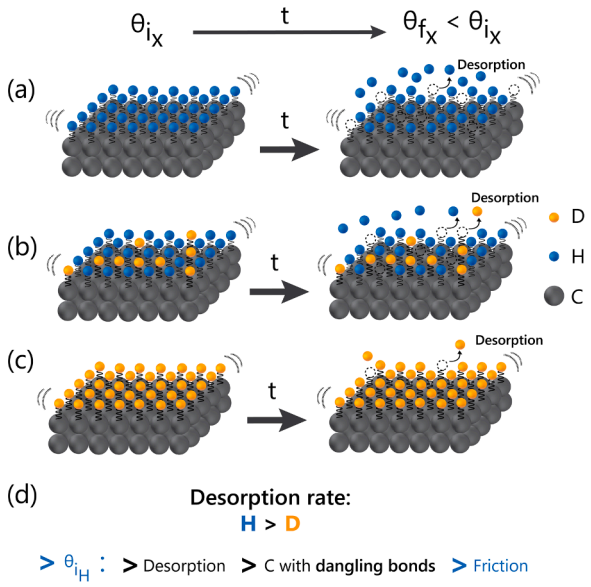

Fig. 8. Schematic of carbon hydrogenated surfaces with H gradually replaced by D, from (a) to (c). After a fixed time, t, the possible dangling bonds at the interface are different depending on the H (or D) content. In (d), the suggested relation is summed up: a higher content of H at the interface may lead to a higher desorption rate of the adsorbates. Consequently, more C atoms with dangling bonds are exposed and susceptible to interaction with the counter body. Finally, as proposed in the model and observed in MD simulations, more active specimens led to higher friction forces, resulting in an indirect isotope mass effect.

passivation.

Considering a generic time *t*, in all the cases the initial coverage fraction of the surface θ_{i_x} will be higher than the final θ_{f_x} because, at the different rates, desorption will take place. However, when comparing the hypothetical samples represented in (a) to (c), the hydrogenated film will have more C atoms available to interaction at the interface after the time *t*, leading to a higher friction force, since the probe-sample interaction will be stronger, as summed up in (d). When deuterium atoms replace hydrogen, the desorption rate and, consequently, the number of active sites, will decrease, until reaching a minimum for a fully-deuterated surface. Accordingly, the deuterated surface may present lower friction than the hydrogenated surface as the lubricity effect attributed to H is also possible to D (since they have similar physical and chemical properties) but the surface coverage is higher. The friction behavior described here supports the isotopic effect due to different desorption rates of isotopes. However, the participation of a third element (dangling bond defects) may make the isotopic effect indirect. The indirect isotopic effect may make clear the complexity of nanoscale events controlling friction and the mandatory integration of mechanisms to fully understand nanofriction in the wearless regime.

Conclusions

Using the premise of different desorption rates for H and D atoms bonded to C atoms due to the difference in the scission energies, it was possible to compare a theoretical approach with experimental results of friction from the bibliography for hydrogenated and/or deuterated amorphous carbon thin films. Based on the coverage percentages from experimental results, a model, based on fundamental properties of both C-H and C-D bonds and thermo-dependent desorption processes, was proposed. The results obtained by using this equation are consistent with the monotonically decreasing friction forces on gradually increasing deuterium coverage on the surface, previously reported by experimental approaches, within the uncertainty of the analysis. In order to support the conclusions, MD simulations were performed to verify the dependency of friction on carbon with the presence of dangling bonds at the interface, simulating a scenario where H and/or D adsorbates are replaced by non-passivated carbon atoms at the interface. Two main points were evidenced: (a) no difference in friction for the H and D covered surfaces was observed, hindering the proposal of a direct isotopic mass effect, and (b) a slight difference of ~ 5% in coverage may be sufficient to evoke an effect as relevant as reported in experimental works. Even though the simulations were carried out in vacuum conditions and very low temperatures to assure total coverage control, in experimental conditions this effect is also expected. Indeed, if the dangling bonds are rapidly suppressed in the experimental setups by blowing ambient air, they will be passivated with chemical species responsible for higher friction forces (for example, oxygenated molecules, as suggested by previous works). Therefore, the dangling bonds generated during the process of desorption, even if suppressed after creation depending on the environmental conditions, could explain the experimental findings. Hence, a tentative indirect isotope effect based on a dynamic equilibrium of different H and D desorption ratios and dangling bond formation (a consequence of the adsorbates' desorption) is here proposed, which merges published experimental results and the simulated condition in the same overall trend. Our work may open new pathways for the integration and convergence of friction mechanisms as phononic friction and van der Waals interactions, since the dangling

bonds or adsorption of chemical specimen leading to higher friction forces may depend on both contributions, and previously reported experimental and theoretical findings. Accordingly, it is a new perspective that integrates old opposite discussions in the scientific literature with new ones but in only one sequence of concepts: isotopic effect – carbon dangling bonds – vdW interactions – phononic dissipation.

Declaration of Competing Interest

The authors declare that they have no known competing financial interests or personal relationships that could have appeared to influence the work reported in this paper.

Acknowledgments

This study was financed in part by the Coordenação de Aperfeiçoamento de Pessoal de Nível Superior – Brasil (CAPES) – Finance Code 001 with PROSUC/CAPES scholarships (L. M. L., D. M. and G. L. R), by Conselho Nacional de Desenvolvimento Científico e Tecnológico (CNPq) - grants 304831/2014-0 and 305253/2018-2 (CAP), 304675/2015-6 and 305528/2018-1 (JEZ), 302370/2015-3 (FA) and 308567/2018-8 (CAF), Programa de Apoio a Núcleos de Excelência (PRONEX), Fundação de Amparo à Pesquisa do Estado do Rio Grande do Sul (FAPERGS) - Project 2019/18460-4 - FAPESP-FAPERGS. This research was also made possible thanks to computational resources provided by the Centro de de Computação Científica (NCC/GridUNESP), Universidade Estadual de São Paulo (UNESP), Núcleo Avançado de Computação de Alto Desempenho (NACAD) da COPPE, Universidade Federal do Rio de Janeiro (UFRJ), and Centro Nacional de Supercomputação, Universidade Federal do Rio Grande do Sul (CESUP/UFRGS).

References

[1] J. Krim, Surface science and the atomic-scale origins of friction: What once was old is new again, Surf. Sci. 500 (2002) 741–758, https://doi.org/10.1016/S0039-6028(01)01529-1.
[2] B. Thomson, An inquiry concerning the source of the heat which is excited by friction, Philos. Trans. R. Soc. Lond. 88 (1798) 80–102, https://doi.org/10.1098/rstl.1798.0006.
[3] H. Bercegol, R. Lehoucq, Vacuum friction on a rotating pair of atoms, Phys. Rev. Lett. 115 (2015) 1–5, https://doi.org/10.1103/PhysRevLett.115.090402.
[4] J.L. Lebowitz, Boltzmann's entropy and time's arrow, Phys. Today 46 (1993) 32–38, https://doi.org/10.1063/1.881363.
[5] M.A. Taye, Effect of viscous friction on entropy, entropy production, and entropy extraction rates in underdamped and overdamped media, Phys. Rev. E. 103 (2021), 042132, https://doi.org/10.1103/PhysRevE.103.042132.
[6] K. Holmberg, A. Erdemir, Influence of tribology on global energy consumption, costs and emissions, Friction 5 (2017) 263–284, https://doi.org/10.1007/s40544-017-0183-5.
[7] S.Y. Krylov, J.W.M. Frenken, The physics of atomic-scale friction: Basic considerations and open questions, Phys. Status Solidi Basic Res. 251 (2014) 711–736, https://doi.org/10.1002/pssb.201350154.
[8] J. Krim, D.H. Solina, R. Chiarello, Nanotribology of a Kr monolayer: A quartz-crystal microbalance study of atomic-scale friction, Phys. Rev. Lett. 66 (1991) 181–184, https://doi.org/10.1103/PhysRevLett.66.181.
[9] B.N. Persson, E. Tosatti, D. Fuhrmann, G. Witte, C. Wöll, Low-frequency adsorbate vibrational relaxation and sliding friction, Phys. Rev. B Condens. Matter Mater. Phys. 59 (1999) 11777–11791, https://doi.org/10.1103/PhysRevB.59.11777.
[10] A. Cammarata, T. Polcar, Control of energy dissipation in sliding low-dimensional materials, Phys. Rev. B 102 (2020) 85409, https://doi.org/10.1103/PhysRevB.102.085409.
[11] A. Cammarata, P. Nicolini, K. Simonovic, E. Ukraintsev, T. Polcar, Atomic-scale design of friction and energy dissipation, Phys. Rev. B 99 (2019) 1–8, https://doi.org/10.1103/PhysRevB.99.094309.
[12] B.N.J. Persson, A.I. Volokitin, Electronic friction of physisorbed molecules, J. Chem. Phys. 103 (1995) 8679–8683, https://doi.org/10.1063/1.470125.
[13] M. Lessel, P. Loskill, F. Hausen, N.N. Gosvami, R. Bennewitz, K. Jacobs, Impact of van der Waals interactions on single asperity friction, Phys. Rev. Lett. 111 (2013), 035502, https://doi.org/10.1103/PhysRevLett.111.035502.
[14] L.M. Leidens, M.E.H. Maia da Costa, N.S. Figueroa, R.A. Barbieri, F. Alvarez, A. F. Michels, C.A. Figueroa, On the physicochemical origin of nanoscale friction: the polarizability and electronegativity relationship tailoring nanotribology, Phys. Chem. Chem. Phys. 23 (2021) 2873–2884, https://doi.org/10.1039/D0CP06436J.
[15] F.G. Echeverrigaray, S.R.S. de Mello, L.M. Leidens, M.E.H. Maia Da Costa, F. Alvarez, T.A.L.L. Burgo, A.F. Michels, C.A. Figueroa, Towards superlubricity in nanostructured surfaces: the role of van der waals forces, Phys. Chem. Chem. Phys. 20 (2018) 21949–21959, https://doi.org/10.1039/c8cp02508h.
[16] R.J. Cannara, M.J. Brukman, K. Cimatu, A.V Sumant, S. Baldelli, R.W. Carpick, Nanoscale friction varied by isotopic shifting of surface vibrational frequencies, Science 318 (80-) (2007) 780–783, https://doi.org/10.1126/science.1147550.
[17] Y. Mo, M.H. Müser, I. Szlufarska, Origin of the isotope effect on solid friction, Phys. Rev. B Condens. Matter Mater. Phys. 80 (2009) 1–7, https://doi.org/10.1103/PhysRevB.80.155438.
[18] S. Kajita, M. Tohyama, H. Washizu, T. Ohmori, H. Watanabe, S. Shikata, Friction modification by shifting of phonon energy dissipation in solid atoms, Tribol. Online 10 (2015) 156–161, https://doi.org/10.2474/trol.10.156.
[19] D. Matté, G.L. Rech, L.M. Leidens, J.E. Zorzi, A.F. Michels, C.A. Figueroa, C. A. Perottoni, Molecular dynamics simulations of the isotopic effect on nanoscale friction, Appl. Phys. A 127 (2021) 657, https://doi.org/10.1007/s00339-021-04803-3.
[20] K.B. Wiberg, The deuterium isotope effect, Chem. Rev. 55 (1955) 713–743, https://doi.org/10.1021/cr50004a004.
[21] B. Gotsmann, M.A. Lantz, Atomistic wear in a single asperity sliding contact, Phys. Rev. Lett. 101 (2008) 1–4, https://doi.org/10.1103/PhysRevLett.101.125501.
[22] F.G. Echeverrigaray, S.R. Sales de Mello, C.D. Boeira, L.M. Leidens, M.E.H. Maia da Costa, F.L. Freire, F. Alvarez, A.F. Michels, C.A. Figueroa, Nanoindentation unidirectional sliding and lateral force microscopy: evaluation of experimental techniques to measure friction at the nanoscale, AIP Adv. 8 (2018), 125013, https://doi.org/10.1063/1.5047801.
[23] S.R.S. De Mello, M.E.H.M. Da Costa, C.M. Menezes, C.D. Boeira, F.L. Freire, F. Alvarez, C.A. Figueroa, On the phonon dissipation contribution to nanoscale friction by direct contact, Sci. Rep. 7 (2017) 1–8, https://doi.org/10.1038/s41598-017-03046-8.
[24] M.E.H. Maia da Costa, F.L. Freire, Deuterated amorphous carbon films: Film growth and properties, Surf. Coat. Technol. 204 (2010) 1993–1996, https://doi.org/10.1016/j.surfcoat.2009.10.011.
[25] T. Kluyver, B. Ragan-Kelley, F. Pérez, B. Granger, M. Bussonnier, J. Frederic, K. Kelley, J. Hamrick, J. Grout, S. Corlay, P. Ivanov, D. Avila, S. Abdalla, C. Willing, Jupyter notebooks – a publishing format for reproducible computational workflows, in: Proceedings of the 20th International Conference on Electronic Publishing (ELPUB 2016), Positioning and Power in Academic Publishing: Players, Agents and Agendas, 2016, pp. 87–90, https://doi.org/10.3233/978-1-61499-649-1-87.
[26] M. Newville, R. Otten, A. Nelson, A. Ingargiola, T. Stensitzki, D. Allan, A. Fox, F. Carter, Michal, D. Pustakhod, Y. Ram, Glenn, C. D., Stuermer, A. Beelen, O. Frost, N. Zobrist, Mark, G. Pasquevich, A.L.R. Hansen, T. Spillane, S. Caldwell, A. Polloreno, Andrewhannum, J. Fraine, deep-42-thought, B.F. Maier, B. Gamari, A. Persaud, A. Almarza, lmfit/lmfit-py 1.0.1, (2020). 10.5281/zenodo.3814709.
[27] E.O. Lebigot, Uncertainties: a Python package for calculations with uncertainties, (2020). https://uncertainties-python-package.readthedocs.io/en/latest/.
[28] I. Levine, Physical Chemistry, 6th ed., McGraw-Hill Education, 2009.
[29] W.M. Haynes, CRC Handbook of Chemistry and Physics, 97th ed., CRC Press, 2016. https://books.google.com.br/books?id=VVezDAAAQBAJ.
[30] K. Gündoğdu, M.W. Nydegger, J.N. Bandaria, S.E. Hill, C.M. Cheatum, Vibrational relaxation of C-D stretching vibrations in CD Cl3, CDBr3, and CDI3, J. Chem. Phys. (2006) 125, https://doi.org/10.1063/1.2361288.
[31] A. Lubezky, L. Chechelnitsky, M. Folman, IR spectra of CH4, CD4, C2H4, C2H2, CH3OH and CH3OD adsorbed on C60 films, J. Chem. Soc. Farad. Trans. 92 (1996) 2269–2274, https://doi.org/10.1039/ft9969202269.
[32] S.H. Lin, B.J. Feldman, Amorphous deuterated-hydrogenated carbon thin-film infrared absorption spectrum, Phys. Rev. B 28 (1983) 413–414, https://doi.org/10.1103/PhysRevB.28.413.
[33] C.A. Figueroa, F. Alvarez, Surface hardness increasing of iron alloys by nitrogen-deuterium Ion Implanting, J. Appl. Phys. 96 (2004) 7742–7743, https://doi.org/10.1063/1.1808887.
[34] J. Atzrodt, V. Derdau, W.J. Kerr, M. Reid, Deuterium- and tritium-labelled compounds: applications in the life sciences, Angew. Chem. Int. Ed. 57 (2018) 1758–1784, https://doi.org/10.1002/anie.201704146.
[35] Z. Chen, A. Khajeh, A. Martini, S.H. Kim, Identifying physical and chemical contributions to friction: a comparative study of chemically inert and active graphene step edges, ACS Appl. Mater. Interfaces 12 (2020) 30007–30015, https://doi.org/10.1021/acsami.0c08121.